Making Rift Valley fever viral particles fluorescent

Yu Gu[1], Jana Koch[1], Céline Garnier[1], Alexandra Erny[1], and Pierre-Yves Lozach[1, †]

From [1]IVPC UMR754, INRAE, Université Claude Bernard Lyon 1, EPHE, PSL Research University, Lyon, F-69007, France

[†]Address correspondence to Pierre-Yves Lozach, pierre-yves.lozach@inrae.fr

Running title: Fluorescent Rift Valley fever virus

i. Abstract

Rift Valley fever virus (RVFV) is a mosquito-borne pathogen that represents a significant threat to both human and veterinary public health. Since its discovery in the Great Rift Valley of Kenya in the 1930s, the virus has spread across Africa and beyond, now posing a risk of introduction into southern Europe and Asia. Despite recent progresses, early RVFV-host cell interactions remain largely uncharacterized. In this methods chapter, we delineate the procedure for labeling RVFV particles with fluorescent organic dyes. This approach makes it feasible to visualize single viral particles in both fixed and living cells and study RVFV entry into host cells. We provide additional examples with two viruses closely related to RVFV, namely Toscana virus and Uukuniemi virus. Furthermore, we illustrate how to utilize fluorescent viral particles to examine and quantify each step of the cell entry program of RVFV, which includes state-of-the-art fluorescence-based detection techniques such as fluorescence microscopy, flow cytometry, and fluorimetry.

ii. Key Words

Bunyavirus, Flow cytometry, Fluorimetry, Intracellular trafficking, Membrane fusion, Microscopy, Phlebovirus, Rift Valley fever virus, Single viral particle tracking, Toscana virus, Uukuniemi virus, Virus entry.

1. Introduction

Over the last decades, significant progresses in fluorescence microscopy and other fluorescence-based techniques have greatly enhanced our comprehension of early virus-host cell interactions. However, our understanding remains largely fragmented. Our knowledge of these intricate processes, which involve hundreds of cellular factors with diverse functions, is confined to a handful of viruses. In this context, we will provide comprehensive protocols to investigate the entry of the phenuivirus Rift Valley fever virus (RVFV) into both fixed and living cells. Initially, we will outline a method for labeling RVFV particles with fluorescent organic dyes. Subsequently, we will introduce a series of experimental procedures to analyze RVFV binding, uptake, intracellular trafficking, and fusion that rely on the use of fluorescently labeled viruses in combination with advanced fluorescence microscopy, flow cytometry, and fluorimetry approaches. To further illustrate our point, we will also employ Uukuniemi virus (UUKV) and Toscana virus (TOSV), two phenuiviruses closely related to RVFV, as examples. The procedures delineated with these viruses can be readily adapted to study not only RVFV but also a wide range of other enveloped viruses.

1.1. The mosquito-borne virus RVFV

RVFV, a bunyavirus of the *Phlebovirus* genus within the *Phenuiviridae* family, predominantly infects livestock and humans [1]. In domestic animals, RVFV can induce fetal malformations, leading to a high rate of abortion and mortality [2]. In humans, the infection can escalate to severe forms, encompassing retinitis, acute hepatitis, hemorrhagic fevers, and encephalitis [2]. RVFV is an arthropod-borne virus (arbovirus) transmitted to vertebrate hosts by a variety of

mosquito species, primarily *Aedes* and *Culex*. Notably, several major RVFV mosquito vectors are expanding to new geographical regions, with some already present in Europe and Middle-East [3].

At the molecular level, RVFV and other phenuiviruses are enveloped viruses, roughly spherical, with an average diameter of 100 nm [4] (Fig. 1). The viral genome consists of three single-stranded RNA segments that are replicated exclusively in the cytosol [5]. The segments, designated as S, M, and L, refer to their respective sizes in nucleic acids, with S the smallest, M the intermediate-sized, and L the largest. Collectively, the three RNA segments code for two non-structural proteins, NSm and NSs, which are absent from viral particles, and four structural proteins, specifically, the RNA-dependent RNA polymerase L, the nucleoprotein N, and the two envelope glycoproteins Gn and Gc. On the viral particle surface, Gn and Gc assemble into an icosahedral lattice of protrusions, exhibiting an atypical T = 12 triangulation [4]. Gn and Gc play crucial roles in virus binding and entry into host cells [6,7].

1.2. Entry of RVFV into host cells

Over the past decade, several receptors for RVFV have been identified (Fig. 2). Heparan sulfates are likely to serve as cell-surface attachment factors [8,9]. The human C-type lectin DC-SIGN acts as a *bona fide* entry receptor for RVFV [10]. The expression of DC-SIGN on the surface of dendritic cells located in the skin dermis, the anatomical site of virus transmission, makes the lectin a compelling candidate for the initial stages of infection. L-SIGN, another C-type lectin present on the surface of the liver endothelium, has been demonstrated to function as an attachment factor and may partially account for the hepatic tropism of the virus [11]. Recently, low-density lipoprotein receptor-related protein 1 (LRP1) was also identified as a viral entry factor [12,13]. Given its broad tissue expression, LRP1 may contribute to the extensive tropism of RVFV [14,15]. However, RVFV can infect tissues

devoid of these receptors, suggesting the virus may utilize alternative receptors, which remain to be identified.

Following virus binding, it has been proposed that a genetically engineered, non-spreading strain of RVFV relies on the clathrin-mediated endocytic pathway for productive entry [16]. In contrast, two reports suggested that the vaccine strain MP12 enters cells independently of clathrin. The first report indicated a role of actin and numerous kinases with functions related to macropinocytosis, proposing that RVFV relies on macropinocytosis for entry [17]. The second study highlighted caveolin, implying that RVFV entry occurs through caveolin-dependent mechanisms [18].

Once internalized, RVFV is sorted into the degradative branch of the endocytic machinery and penetrates into the cytosol via acid-activated membrane fusion from late endosomes. The crystallographic structure of the ectodomain of the RVFV Gc protein has been obtained in its two states, pre- and post-fusion, with a resolution of less than 2.0 Å [19,20], indicating that Gc is a class II membrane fusion protein [7]. Upon endosomal acidification, the two RVFV glycoproteins Gn and Gc undergo multiple conformational changes, leading to the fusion of the viral envelope with the endosomal membranes [21]. While acidification below pH ~5.7 is sufficient to trigger RVFV fusion [16], the overall process depends on additional factors such as the lipid composition of target membranes, most of which remain to be identified.

1.3. Utilization of small fluorescent dye molecules for viral particle labeling

The fluorescent labeling of viral particles constitutes a critical initial step in any methodology aimed at visualizing viruses and tracking single viral particles during their entry process. In 2018, we contributed to a book on Influenza Virus within the series “Methods in Molecular Biology”, with a chapter focusing on the fluorescent labeling of viral particles using UUKV as a model virus system [22]. Since then, a variety of novel methods have been developed to

render viral particles fluorescent [23]. Many of these have been applied to bunyaviruses, but to our knowledge, none to RVFV [24]. One such method involves the genetic engineering of viruses to carry fluorescent protein reporters or stainable small tags such as clickable amino acids [25], which exhibits a minimal invasiveness, or the tetracysteine peptide with biarsenical fluorescent compounds [26]. Fluorescent organic dyes are also commonly employed to non-specifically stain structural proteins, nucleic acids, and envelope membranes in viral particles. Inorganic dyes have been used as well to confer fluorescence to viruses [27]. Each of these approaches has its own set of advantages and disadvantages, as discussed in these recent reviews [24,23,28].

In this chapter, our focus will be on describing experimental procedures that employ fluorescent organic dyes. Despite the availability of numerous organic dyes [28], we will limit our presentation to two specific ones: octadecyl rhodamine B chloride (R18) and Alexa Fluor (AF) molecules (Fig. 1 and Table 1). Multiple variants of AF molecules exist. Some are thiol-reactive, *i.e.*, they form covalent bonds with free cysteine residues in the protein targeted for labeling, while others react with free amine groups. Only the latter will be addressed here. Collectively, these dyes are characterized by their bright fluorescence, high photostability, and a broad range of emission colors, spanning from ultraviolet to far red. Such labeling is arguably the least invasive and most compatible with the analysis of both fixed and living cell samples.

AF molecules are commonly employed for the fluorescent labeling of viral particles. They react with free amine residues in the viral transmembrane proteins such as RVFV Gn and Gc. This approach paves the way for tracking single viral particles, thereby enabling the monitoring of virus binding, uptake, and intracellular trafficking. The dye R18 is lipophilic and typically utilized to label the envelope of viral particles, given its propensity to insert into lipid bilayers. A high concentration of R18 dye molecules within the virus envelope results in the auto-quenching of the fluorescence signal. In this respect, R18 proves to be an invaluable asset

for assessing and quantifying viral membrane fusion. Fusion events result in the release of R18 into the endosomal membrane, leading to a subsequent increase in fluorescence that can be quantified with a fluorometer (Fig. 2).

1.4. Fluorescence microscopy to track virus entry events

Upon labeling, the fluorescence associated with the viral particles necessitates visualization. For this purpose, fluorescence microscopy is an evident first choice for imaging virus entry. Laser scanning confocal microscopy facilitates internal imaging by scanning multiple focal planes from the bottom to the top of a cell. Derivative technologies have enabled ultrafast confocal imaging, such as spinning disc microscopy, which are particularly suited to studying the dynamics of virus entry into cells. Total internal reflection fluorescence (TIRF) microscopy serves as another example. TIRF microscopy enables the visualization of the plasma membrane and virus motion at the cell surface with remarkable precision [29,10]. Super-resolution microscopy, as well as correlative light and electron microscopy (CLEM), provide access to nanoscale details of virus penetration into cells. Light-sheet microscopy and multiphoton microscopy are poised to potentially enable the tracking of virus entry in thick samples, such as live animals, in the near future [30]. For a more comprehensive understanding of these microscopy techniques, we recommend recent reviews [31-35].

1.5. Quantification and definition of the primary steps in virus entry

The emergence of computer-assisted image analysis and artificial intelligence-driven deep-learning algorithms has enabled the large-scale quantification of microscopy images. The convergence of these technologies has greatly accelerated research into how viruses enter their host cells [36,37]. In many instances, flow cytometry and fluorimetry serve as interesting alternatives for measuring virus binding, internalization, and fusion. Both methods provide a good compromise between the number of samples to be analyzed and the speed of analysis. Moreover, fluorescently labeled viral particles can be employed in combination with the use of

perturbants of the endocytic machinery such as drugs, dominant negative and constitutively active mutants, and gene silencing. Additionally, cells can also be transfected with plasmids encoding endocytic markers fused to fluorescent proteins prior to virus exposure and subsequent analysis [38]. Altogether, these approaches have proven instrumental in providing new insights into the entry routes used by several bunyaviruses closely related to RVFV [24].

2. Materials

2.1. Virus production

1. 175-cm² cell culture flasks equipped with filter screw caps.

2. Dulbecco's Minimum Essential Medium (DMEM).

3. Glasgow's Minimum Essential Medium (GMEM).

4. Vero African green monkey kidney epithelial cells cultured in DMEM, supplemented with 10% (v/v) fetal bovine serum (FBS) and 1% (v/v) penicillin/streptomycin.

5. BHK-21 baby hamster kidney cells cultured in GMEM, supplemented with 5% (v/v) FBS, 10% (w/v) tryptose phosphate broth, 1% (v/v) penicillin/streptomycin.

6. Phosphate-buffered saline (PBS).

7. Trypsin-ethylenediaminetetraacetic acid (EDTA).

8. RVFV ZH548, a strain isolated from human cases in Egypt [39].

9. TOSV H4096, a strain from the B lineage of Toscana virus [40].

10. UUKV S23, the prototype strain of UUKV [41,42].

11. Standard 50-mL tubes.

12. An ultracentrifuge and a rotor with buckets equivalent to the SW28 or 32 (Beckman Coulter).

13. Ultracentrifuge tubes compatible with the SW28 or 32 buckets.

14. Sucrose.

15. 4-(2-hydroxyethyl) piperazine-1-ethanesulfonic acid (HEPES).

16. 10× HNE buffer (100 mM HEPES, 1.5 M NaCl, 10 mM EDTA), filtered through a 0.2 µm filtration membrane. The stock solution can be stored at room temperature (RT) for an extended period.

17. 25% (w/v) sucrose solution: first, dilute 25 g of sucrose in 50 mL of deionized water, then supplement with 10 mL of 10× HNE buffer, and finally complete to 100 mL with sterile water. Filter the solution through a 0.2 µm filtration membrane.

18. Prepare 1× HNE buffer by diluting the 10× stock solution 1:10 in sterile water.

19. Cut pieces (approximately 3 cm × 3 cm) of Parafilm "M" (Laboratory Film).

2.2. Labeling of viral particles with fluorescent dyes

1. Precast 4-12% Bis[Tris(hydroxymethyl)aminomethane] (Bis-Tris) 10-well gels (Thermo Fisher Scientific).

2. 3-(N-morpholino) propanesulfonic acid (MOPS) sodium dodecyl sulfate (SDS) running buffer (Thermo Fisher Scientific).

3. Any protein blue loading buffer. The one used here is the 4× lithium dodecyl sulfate (LDS) sample buffer (Thermo Fisher Scientific).

4. Gel fixative solution [40% (v/v) methanol and 10% (v/v) acetic acid)].

5. Coomassie blue staining solution [50% (v/v) methanol, 10% (v/v) acetic acid, and 0.25% (w/v) Serva Blue G (Serva)].

6. Ultrapure bovine serum albumin (BSA).

7. AF and R18 dyes (all from Thermo Fisher Scientific). Resuspend the working stocks in dimethyl sulfoxide for AF dyes and 100% ethanol for R18 according to the manufacturer's recommendations. Aliquot and store at -80 °C.

8. Sucrose.

9. An ultracentrifuge and a rotor with buckets equivalent to the SW60 (Beckman Coulter).

10. Ultracentrifuge tubes compatible with the SW60 buckets.

2.3. Characterization of fluorescently labeled viral particles

1. Any classical 6-well plates.

2. Vero cells.

3. DMEM supplemented with 2% FBS, 1% (v/v) penicillin/streptomycin.

4. Agarose solution A: dissolve 2% agarose in deionized water by microwave heating. Maintain at 60 °C in an incubator.

5. Agarose solution B: 40% (v/v) DMEM, 4% (v/v) FBS, 5.9% (v/v) sodium bicarbonate [7.5% (v/v) stock, Gibco], 0.2% (v/v) penicillin/streptomycin, and 2% (v/v) glutamine (100× stock, Gibco). Maintain at 50 °C in a water bath.

6. PBS.

7. Prepare fixative buffer [4% (w/v) formaldehyde (FA)].

8. A 0.2 % crystal violet solution.

9. Precast 4-12 % Bis-Tris 10-well gels (Thermo Fisher Scientific).

10. Any protein blue loading buffer. The one used here is the 4× LDS sample buffer (Thermo Fisher Scientific).

11. A fluorescence imaging system such as the Odyssey imaging system.

12. Microscope slides (76 × 26 × 1 mm, Marienfeld).

13. 12-mm microscope cover glasses (Thermo Fisher Scientific).

14. Any confocal microscope.

15. Any wide-field microscope.

2.4. Analysis of virus entry by fluorescence microscopy

1. Various models of Nunc Lab-Tek chambers (Thermo Fisher Scientific), with unique or multiple wells, suitable for both fixed and live-cell microscopy analysis (*see* **Note 1**).

2. Phenol red-free DMEM.

3. Binding buffer [phenol red-free DMEM supplemented with 0.2 % (w/v) BSA and 20 mM HEPES (pH ~7.4)].

4. Any spinning disc or confocal microscope with live-cell imaging capabilities.

5. Any wide-field microscope with live-cell imaging capabilities.

6. A549 human lung epithelial cells cultured in DMEM supplemented with 10 % (v/v) FBS and 1 % (v/v) MEM non-essential amino acids (Thermo Fischer Scientific).

7. Opti-MEM I (Thermo Fischer Scientific).

8. Lipofectamine 2000 (Thermo Fischer Scientific).

9. pcDNA3 plasmid coding for PH-PLCΔl-EGFP, a fluorescent protein marker in the plasma membrane conjugated to the enhanced green fluorescent protein (EGFP), or an equivalent plasmid system coding for fluorescent plasma membrane marker.

10. EDTA.

11. Extracellular matrix (ECM) obtained by detaching cells with EDTA.

12. Any TIRF microscope that allows the illumination of the bottom surface or cytoplasm of live cells by adjusting the penetration depth between 90 and 200 nm.

13. Human cervical carcinoma epithelial cells HeLa cultured in DMEM supplemented with 10 % (v/v) FBS.

14. Fixative buffer.

2.5. Analysis of virus entry by flow cytometry and fluorimetry

1. U-bottom 96-well plates without cell culture treatment.

2. Binding buffer.

3. Fixative buffer.

4. PBS.

5. A549 cells.

6. Trypan Blue.

7. Any flow cytometer equipped with a blue laser.

8. Standard 1.5-mL tubes.

9. Any high-sensitivity spectrofluorometer. Here, an FP-8550 fluorometer (Jasco) equipped with a water bath was used.

3. Methods

3.1. Virus production

1. Propagate cells to approximately 60-80 % confluency within 35 mL of complete growth medium in 175-cm² cell culture flasks (*see* **Note 2**). Use PBS for cell wash steps and Trypsin-EDTA solution for the detachment of cells, as is standard for cell passaging of adherent cells.

2. Wash cells once with serum-free media before exposure to the virus in 15 mL of serum-free medium per flask at a multiplicity of infection (MOI) of 0.01 for 1 h at 37 °C (*see* **Note 3**).

3. Discard the input virus and replace it with 35 mL of serum-free medium per flask (*see* **Note 4**).

4. Incubate infected cells at 37 °C for up to 72 h (*see* **Note 5**).

5. Harvest the 35 mL of virus-containing supernatant and collect in 50 mL tubes. Then clear the supernatant by centrifugation at 2000 × g for 20 min at 4 °C (*see* **Note 6**).

6. Pool the virus-containing supernatants and distribute 33.5 mL per SW28/32 tube. Carefully underlay the supernatant with 2.5 mL of 25 % (w/v) sucrose solution (*see* **Note 7**).

7. Concentrate the viral particles by ultracentrifugation at 100000 × g at 8 °C for 2 h (acceleration and deceleration set to maximum) (*see* **Note 8**).

8. After ultracentrifugation, dispose the supernatant. Immediately add 300 µL of HNE buffer to each tube and cover with parafilm to prevent the virus pellets from drying. Allow the pellets to dissolve on ice for at least 1 h (*see* **Note 9**).

9. Gently resuspend the virus pellets by pipetting up and down several times on ice.

10. Pool the resuspended virus and make aliquots for long-term storage at -80 °C (*see* **Note 10**).

3.2. Labeling of viral particles with fluorescent dyes

1. The viral glycoproteins Gn and Gc in the virus stock are first semi-quantified through SDS-polyacrylamide gel electrophoresis (PAGE) separation, followed by Coomassie blue staining. Mix varying amounts of viral proteins (typically 15, 10, and 5 µL of the virus stock) with LDS sample buffer to a final volume of 20 µL. Then, separate the proteins by SDS-PAGE through a 10-well precast 4-12 % Bis-Tris gradient gel using a MOPS SDS running buffer.

2. Incubate gels in the fixative buffer for 1 h before staining with the Coomassie solution for up to 12 h, followed by extensive washing with water (*see* **Note 11**). An example for RVFV is shown in Fig. 3a.

3. The glycoproteins Gn and Gc are normalized against BSA. Measure the intensity of each band with the ImageJ software [43]. To this end, define one square and used it to measure each band, as illustrated in Fig. 3a (box1). Use an empty well (labeled "0" in Fig. 3a) to define the background level, and subtract this value from all other values. Define a linear regression curve to correlate the relative unit (RU) and the quantity of protein (Fig. 3b). By applying the equation of the linear regression curve, it is possible to determine the quantity of Gn and Gc in each sample (Table 2).

4. Add AF dyes in a range of 1:1 - 1:5 molar ratio of viral envelope glycoproteins to dye while vortexing (*see* **Note 12**). Alternatively, label 10^9 infectious viral particles, as determined by plaque-forming unit (pfu) assay, with the lipid dye R18 (20 µM) according to a similar protocol. Incubate at RT for 2 h in the dark whilst gently mixing on a shaker.

5. Band the fluorescently labeled particles in a sucrose density gradient composed of four steps, prepared in ultracentrifuge SW60 tubes. For each step, carefully pipette 900 µL of sucrose with a final (v/v) concentration of 15%, 30%, 45%, and 60% on top of each other, starting with the

highest concentration. After each layer, the tubes are placed at -80 °C until the solutions are frozen. Thaw the gradients overnight at 4°C to allow linearization of the gradient.

6. Gently overlay the dye-virus mix (from step 4) onto the gradient. Centrifuge at 100000 × g at 4 °C for 90 min (acceleration and deceleration set to maximum and minimum respectively). Subsequently, viral particles exhibiting identical density are typically observed to concentrate within the 35-40% sucrose range. Unbound dyes usually remain at the top of the gradient (Fig. 4a) (*see* **Note 13**).

3.3. Characterization of fluorescently labeled viral particles

3.3.1. Virus titration by pfu assay

1. Seed Vero cells in 6-well plates (5×10^5 cells per well) 18 h before infection by RVFV and TOSV. To determine the infectious titer of UUKV, please *see* **Note 14**.

2. On the day of infection, ensure that cells form confluent monolayers. Wash cells with serum-free medium.

3. Add 200 µL of 10-fold dilutions of viral particles in serum-free medium (from 10^{-2} to 10^{-8}) to the wells. On top, add 800 µL of serum-free medium per well. Incubate at 37 °C for 1 h.

4. During the incubation, gently mix Agarose solution A with Agarose solution B in a water bath warmed at 50 °C. Once the agarose solution (A+B) cold down to 40-43 °C, add 4 mL of the solution per well. Then return the plate to an incubator at 37 °C.

5. Wait until the agarose layer hardens, which typically requires at least 1 h, and turn the plate upside down to prevent water droplets resulting from condensation on the lid from falling onto the agarose surface. Incubate at 37 °C for 4 days.

6. Remove the agarose with a cone tip by inserting it between the plastic edge of the well and the agarose layer. Fix the cells with fixative buffer for at least 2 h.

7. Wash cells with PBS. Then stain cells with 0.2 % crystal violet for 20 min.

8. Thoroughly, but carefully, rinse the cells with water and allow them to dry at RT. The titer of virus (pfu.mL^{-1}) is obtained by counting the number of pfu (n) at a factor of dilution (f) for which n is comprised between 3 and 30 using the equation $5 \times n / f$. In the example shown in Fig. 4b, one can count 19 pfu at the dilution 10^{-7}. Therefore, the titer of this AF546-labeled RVFV stock is $5 \times 19 / 10^{-7} = 9.5 \times 10^{8}$ pfu.mL^{-1}.

3.3.2. Assessing integrity of labeled viruses

1. To control for the intactness of fluorescent viruses, dilute viral particles in LDS sample buffer and separate the viral proteins by SDS-PAGE in 10-well precast gradient gels.

2. Expose the gel to a fluorescence imaging system. Only Gn and Gc should be fluorescently labeled (Fig. 4c). The absence of fluorescent signal from the nucleoprotein N indicates that the viral envelope is intact.

3.3.3. Visualization of viral particles

Analyze fluorescently labeled viral particles by microscopy to confirm the homogeneity of the viral preparation and ensure the absence of aggregates. Add 5 µL of a fluorescently labeled virus preparation onto a microscopy slide and gently place a coverslip on top. Fig. 4d is an illustration of AF546-labeled RVFV (RVFV-AF546) imaged by confocal microscopy and shows both single viral particles and clusters of particles. Of note, wide-field microscopy with a magnification of 20× is usually sufficient to visualize the particles and detect potential aggregates.

3.4. Analysis of virus entry by fluorescence microscopy

3.4.1. Live-cell imaging using wide-field and confocal fluorescence microscopy

1. Seed cells in 8-well Nunc Lab-Tek chambers (2.5×10^{4} cells per well in 400 µL of complete medium) (*see* **Note 15**) and incubate at 37 °C overnight.

2. The next day, wash cells once with phenol red-free binding buffer and cover the wells with 400 µL of the said pre-warmed binding buffer at 37 °C for 30 min.

3. Transfer the Nunc Lab-Tek chambers on the stage of the microscope (*see* **Note 16**).

4. Add the fluorescently labeled viral particles into the well when the confocal microscope is set up and ready for imaging (*see* **Note 17**). Fig. 5a illustrates RVFV-AF546 on filopodia monitored with a confocal microscope, highly likely surfing towards the cell body before endocytosis into Vero cells. In these examples, cells were reverse-transfected with a plasmid carrying the gene for PH-PLCΔ1-EGFP, an EGFP-tagged protein associated with the plasma membrane. DNA transfection was performed 24 h prior to imaging using Opti-MEM I and Lipofectamine 2000 according to the manufacturer's recommendation.

3.4.2. Live-cell imaging by TIRF microscopy

1. To track fluorescent viral particles using TIRF microscopy, two methods can be applied to localize viral particles between the cells and coverslip (*see* **Note 18**).

   (a) In the first case, cells are detached from the culture plate with EDTA and exposed to the virus in suspension in phenol red-free binding buffer on ice. Virus-bound cells are then seeded on coverslips and immediately imaged (*see* **Note 19**).

   (b) The second case involves pre-binding of viral particles to coverslips coated with ECM and seeding of cells on top of the bound viral particles (*see* **Note 20**).

2. A TIRF microscope is used to illuminate the bottom surface or cytoplasm of live cells by adjusting the penetration depth at 90 and 200 nm, respectively. Trajectories and fluorescence intensity of virus spots are analyzed by computational analysis with the Image J-based plugin software Particle Tracker (http://imagej.net/Particle_Tracker) [44]. An example of the trajectory of UUKV labeled with AF647 (UUKV-AF647) on HeLa cells expressing the virus receptor DC-SIGN (Hela-DC-SIGN) [10] is shown in Fig. 5b.

3.4.3. Live cell imaging to monitor virus binding and internalization

1. Seed cells in 8-well Nunc Lab-Tek chamber (2.5×10^4 cells per well in 400 µL of complete medium) and incubate at 37 °C overnight (*see* **Note 21**).

2. The following day, wash cells once with binding buffer and expose the cells to the desired MOI of fluorescently labeled viral particles diluted in 200 µL binding buffer on ice for 2 h.

3. Wash cells with pre-chilled binding buffer. Rapidly warm to 37 °C by adding 400 µL pre-warmed complete medium and incubate within the pre-warmed chamber of a classical or ultrafast confocal microscope (*see* **Note 22**).

4. Warming the cells reactivates endocytosis and allows the virus to enter. The imaging must therefore start immediately after the temperature rises (*see* **Note 23**). Fig. 5c depicts UUKV labeled with AF568 (UUKV-AF568) bound to the surface and subsequently internalized into the cytoplasm of HeLa-DC-SIGN cells.

3.5. Analysis of virus entry by flow cytometry and fluorimetry

3.5.1. Virus binding

1. Perform binding assays in 96-well plates with U-bottom using 2×10^5 cells in 200 µL of binding buffer (*see* **Note 24**).

2. Pellet cells by centrifugation (300 × g, 4 °C, 5 min) and replace the binding buffer by fluorescently labeled viral particles at desired concentrations in 100 µL of binding buffer. This step is carried out at 4 °C with gentle agitation for 2 h.

3. Remove unbound viral particles by a single wash with 200 µL of binding buffer and resuspend cell pellets in 100 µL of 4% (w/v) FA in PBS for 20 min at 4 °C.

4. Wash cells once with PBS before flow cytometry analysis. To illustrate this approach, a quantification of the binding of AF488-labeled TOSV (TOSV-AF488) to A549 cells is shown in Fig. 6a.

3.5.2. Virus internalization

1. For internalization assays, bind AF488-labeled viral particles to cells as described above.

2. After 2 h on ice, wash cells with pre-chilled binding buffer to remove unbound particles.

3. Rapidly warm infected cells at 37 °C by resuspension in pre-warmed binding buffer supplemented with 5 % (v/v) FBS to allow virus internalization and keep the cells at 37 °C for the required time period (*see* **Note 25**).

4. To stop internalization, put cells back on ice until flow cytometry analysis.

5. To distinguish between internalized and surface-bound particles, add Trypan Blue to the cells at a final concentration of 0.04 % (w/v) for 15 sec and immediately process the sample in the flow cytometer [45]. Trypan Blue is membrane impermeable and thus only able to quench the fluorescence of green viral particles still exposed on the cell surface. Fig. 6b is an example of analysis showing the internalization of TOSV-AF488 into HeLa-DC-SIGN cells.

3.5.3. Viral fusion

1. Our approach to analyze acid-activated virus membrane fusion from endosomes depends on the auto-quenching properties of the lipid dye R18 [36]. This method allows for accurate quantification of virus fusion with endosomal membranes in living cells (*see* **Note 26**).

2. Expose one million of cells to R18-labeled viruses at a MOI of 5 in 1.5-mL tubes containing 500 µL of binding buffer and incubate on ice for 1 h (*see* **Note 27**).

3. After binding, pellet and wash the cells once with pre-chilled binding buffer at 4 °C.

4. Resuspend the cells in pre-warmed complete phenol red-free medium at 37 °C to trigger virus internalization, and immediately transfer the cells inside the spectrofluorometer at 37 °C while measuring the fluorescence in real-time (*see* **Note 28**). Fig. 7 illustrates the monitoring of penetration of TOSV labeled with R18 (TOSV-R18) into A549 cells by measuring the dequenching of the dye R18 with a spectrofluorometer.

4. Notes

1. Alternative cell chambers to Nunc Lab-Tek are available on the market, such as Ibidi cell culture dishes with or without culture inserts and MatTek culture slides and dishes.

2. To achieve a confluence of 70-80 % the next day (roughly 24 h), about 10-15 and 15-20 million of Vero and BHK-21 cells, respectively, are seeded. To obtain a homogenous distribution of cells over the entire flask, keep the flasks on a flat surface, such as a bench, for 5-10 min before incubation at 37 °C. Very often, shelves in incubators are not perfectly flat. It is recommended to use seven flasks, one of which is used as a mock-infected control to detect cytopathogenic effect (CPE) by comparison with infected flasks. The total volume of 6 flasks corresponds to the maximal volume that can be loaded into SW28/32 buckets for one round of ultracentrifugation.

3. Move the flasks back and forth every 10 min. This will minimize the risk that cells drying out due to the low volume used for infection.

4. Vero and BHK-21 cells can be cultured in the absence of serum for several days. This represents an advantage in facilitating the subsequent purification of the viral particles required for the labeling procedure.

5. To preserve the newly produced viral particles, it is important to harvest the supernatant before infected cells die. Typically, CPE appears in cells infected by phenuiviruses at a MOI of 0.01 48-72 h post-infection. During this period, cells must be carefully monitored to collect the virus at the most appropriate moment, *i.e.*, just when cells start to detach from the plastic. The timing can vary greatly from one virus to another, and for a specific virus, from one production to another, and must be seriously taken into consideration to establish an efficient protocol of production.

6. RVFV and other phenuiviruses support several cycles of freezing – thawing without altering the infectivity of the viral particles. It is therefore possible to stop the protocol at this step by adding 10 mM final concentration of HEPES and store the supernatant either at 4 °C overnight or -80 °C for a longer period. In the latter case, the thawing step must be done slowly at RT.

HEPES helps to buffer the supernatant at neutral pH and protect viral particles against the drop in pH during the freezing – thawing steps.

7. It is recommended to aspirate a higher volume of 25 % (w/v)-sucrose solution with a 5-mL pipette than required to underlay the supernatant in the ultracentrifuge tube. This helps to avoid refluxes of supernatant in the pipette during the procedure, and in turn, facilitates the formation of a well-defined sucrose cushion. In addition, the sucrose cushion is made in the same buffer as used to resuspend the virus pellet.

8. The velocity of ultracentrifugation depends on the biophysical properties of the virus studied (density, volume, etc.).

9. After pouring out the supernatant, excess liquid can be absorbed from the upper rim of the centrifugation tubes with paper. Avoid contacting the virus pellet during this step. Optionally, but also depending on the virus produced, the pellets can be dissolved on ice overnight. Finally, virus pellets can also be resuspended in other buffers than HNE, *e.g.*, Tris-based buffer. However, HNE is preferred for labeling with AF dyes. These dyes react with free amines, which are present in large amounts in the Tris buffer itself. This can result in a lower efficiency of the labeling procedure.

10. It can happen that white aggregates float in suspension after resuspension of the virus pellets, depending on the cell type and culture media products used. These aggregates can be easily removed by an additional centrifugation step at 3000 × g for 15 min at 4 °C.

11. A washing solution of 10 % (v/v) acetic acid can also be used for a more efficient destaining. Note that phenuivirus glycoproteins generally appear with a better focus after SDS-PAGE and Coomassie blue staining when they are not reduced.

12. Cautionary steps should be taken to ensure that viral infectivity is not impaired by the labeling, which typically happens when a high molar ratio of viral envelope glycoproteins to

dyes is used (>1:10). This ratio usually depends on the number of amine groups on the viral envelope glycoproteins that are free to react with the dye molecules. For instance, a high number of free amine groups in the phenuivirus glycoproteins Gn and Gc makes it possible to get bright fluorescent viral particles with a relatively low quantity of dyes (ratio 1:1), and nearly no impact on viral infectivity. Furthermore, the choice of the dye color depends on the purpose and constraint/restrictions of each experiment involving fluorescent viral particles.

13. To see a virus band in gradients by eye, a minimal amount of 100 µg of Gn/Gc must be loaded. Below this quantity, it is extremely difficult to see the virus band. In this latter case, collect fractions from the gradient and assess each of them for the presence of fluorescently labeled virions, *e.g.*, by western blot analysis against viral proteins. Furthermore, the percentage in sucrose for each step as well as the velocity of ultracentrifugation might be adjusted according to the biophysical properties of the virus studied.

14. Pfu assay is suitable for lytic virus, such as RVFV and TOSV. However, for non-lytic virus like UUKV, the titration can be achieved by foci-forming unit assay. This procedure has been described in detail in a chapter dedicated to UUKV in the Methods in Molecular Biology series [22].

15. Imaging of isolated, single cells is usually easier for tracking viral particles in cells. For this reason, a relatively low number of cells is seeded the day before the experiment.

16. For live-cell imaging, it is recommended to use a microscope equipped with a chamber that allows for the control of temperature, carbon dioxide, and humidity.

17. Usually, the volume of fluorescently labeled viral particles is negligible in comparison with the volume of medium in the well. Depending on the virus analyzed, it can take up to several minutes before the viral particles sediment and attach to the cells. Alternatively, it is possible to synchronize the binding on ice before warming and imaging. The disadvantage of this latter

method is that (1) a thermal shock can result in difficulties to get the right focus, and (2) it requires to set up the microscope very rapidly to not miss the early steps of virus internalization.

18. For the visualization of cell-bound particles by TIRF microscopy, the virions have to be localized between the cell and the coverslip. Small viruses such as murine polyomavirus can diffuse into this narrow space, but larger viruses such as RVFV and other phenuiviruses do not. Therefore, for small viruses, it is possible to seed the cells the day prior infection and microscopy analysis. The viral particles can be added directly in the well at 37 °C inside the environmental chamber of the microscope. This has the advantage to enable the presetting of the microscope for imaging before adding the virus.

19. Imaging starts when cells come into contact with the glass surface, which can take a few minutes. Furthermore, one technical issue is that it takes a minimum of 5 min to set up the TIRF microscope and start recording. This means that reactions at 37 °C are already well on their way before recording starts. To slow down the process, imaging can be performed at RT.

20. To attach viruses on coverslips prior to TIRF microscopy, coverslips are coated with ECM [46]. This simply consists of seeding cells on the coverslips and detaching them with EDTA a few days later. The ECM remains on the coverslips. Alternatively, fibronectin or polylysine can be used to pre-coat coverslips and attach viral particles.

21. For the same reasons as exposed in **Note 15**, only a low number of cells is seeded the day before infection and imaging.

22. The choice of a classical or ultrafast confocal microscope, *i.e.*, spinning disc microscope, depends on the purpose of the experiment. An ultrafast confocal microscope is particularly appropriate for live-cell imaging. Such a microscope is also substantially faster than a normal scanning confocal microscope for the analysis of fixed samples when large series of z-stacks and many fields must be imaged.

23. The timing for penetration depends on the virus studied. It can vary greatly, from a few minutes, *e.g.*, Semliki Forest virus, to hours, *e.g.*, human papillomavirus.

24. Both non-adherent and adherent cells can be employed in this assay. When adherent cells are used, they are first detached from their plastic culture flasks by treatment with 0.5 mM EDTA in PBS at 37 °C for 10 min. Cells are then extensively washed to get rid of EDTA and incubated in complete medium at 37 °C for 30 min. This step helps cells to recover from EDTA treatment. Wash cells at least twice with binding buffer before distribution into 96-well plates.

25. The first 10 min of warming have to be performed in a water bath. Thermal conduction is much more efficient in water than in the air, and therefore, enables faster warming of the samples. Results can significantly vary if warming is done in a regular incubator. Depending of the virus studied, the presence or absence of serum during the warming step must be carefully considered. This is because it can impact the virus internalization process at large.

26. This approach can also be applied to study fusion with liposomes.

27. This assay can involve the use of both non-adherent and adherent cells. For studies with adherent cells, see **Note 24**. Moreover, infection of cells with a lower MOI is possible. In this latter case, it is recommended to increase the number of cells to keep a level of total fluorescence sufficiently high to be measured by fluorimetry.

28. For live-cell measurements, it is important to stir the cells with a magnet. Otherwise, cells will sediment on the bottom of the fluorimeter cuvette. As explained in **Note 25**, the use of serum for the virus internalization should be carefully considered. Alternatively, virus internalization can be performed in a water bath. Cells can be then kept on ice to block endocytosis. This approach presents the advantage to allow measuring all samples at the same time. Finally, as explained in **Note 23**, the timing of internalization depends on the virus that is investigated.

Acknowledgments

This work was supported by INRAE and Agence Nationale de la Recherche fundings (ANR, 21-CE11-0012 and 22-CE15-0034), all awarded to P.Y.L.

References

1. Xu Y, Wang X, Jiang L, Zhou Y, Liu Y, Wang F, Zhang L (2023) Natural hosts and animal models for Rift Valley fever phlebovirus. Front Vet Sci 10:1258172. doi:10.3389/fvets.2023.1258172

2. Wright D, Kortekaas J, Bowden TA, Warimwe GM (2019) Rift Valley fever: biology and epidemiology. The Journal of general virology 100 (8):1187-1199. doi:10.1099/jgv.0.001296

3. Lumley S, Horton DL, Hernandez-Triana LLM, Johnson N, Fooks AR, Hewson R (2017) Rift Valley fever virus: strategies for maintenance, survival and vertical transmission in mosquitoes. The Journal of general virology 98 (5):875-887. doi:10.1099/jgv.0.000765

4. Freiberg AN, Sherman MB, Morais MC, Holbrook MR, Watowich SJ (2008) Three-dimensional organization of Rift Valley fever virus revealed by cryoelectron tomography. J Virol 82 (21):10341-10348. doi:10.1128/JVI.01191-08

5. Peng K, Lozach PY (2021) Rift Valley fever virus: a new avenue of research on the biological functions of amyloids? Future Virol 16 (10):677-689. doi:10.2217/fvl-2021-0094

6. Koch J, Xin Q, Tischler ND, Lozach PY (2021) Entry of Phenuiviruses into Mammalian Host Cells. Viruses 13 (2). doi:10.3390/v13020299

7. Spiegel M, Plegge T, Pohlmann S (2016) The Role of Phlebovirus Glycoproteins in Viral Entry, Assembly and Release. Viruses 8 (7). doi:10.3390/v8070202

8. de Boer SM, Kortekaas J, de Haan CA, Rottier PJ, Moormann RJ, Bosch BJ (2012) Heparan sulfate facilitates Rift Valley fever virus entry into the cell. J Virol 86 (24):13767-13771. doi:10.1128/JVI.01364-12

9. Riblett AM, Blomen VA, Jae LT, Altamura LA, Doms RW, Brummelkamp TR, Wojcechowskyj JA (2016) A Haploid Genetic Screen Identifies Heparan Sulfate Proteoglycans

Supporting Rift Valley Fever Virus Infection. J Virol 90 (3):1414-1423. doi:10.1128/JVI.02055-15

10. Lozach PY, Kuhbacher A, Meier R, Mancini R, Bitto D, Bouloy M, Helenius A (2011) DC-SIGN as a receptor for phleboviruses. Cell host & microbe 10 (1):75-88. doi:10.1016/j.chom.2011.06.007

11. Leger P, Tetard M, Youness B, Cordes N, Rouxel RN, Flamand M, Lozach PY (2016) Differential Use of the C-Type Lectins L-SIGN and DC-SIGN for Phlebovirus Endocytosis. Traffic 17 (6):639-656. doi:10.1111/tra.12393

12. Ganaie SS, Schwarz MM, McMillen CM, Price DA, Feng AX, Albe JR, Wang W, Miersch S, Orvedahl A, Cole AR, Sentmanat MF, Mishra N, Boyles DA, Koenig ZT, Kujawa MR, Demers MA, Hoehl RM, Moyle AB, Wagner ND, Stubbs SH, Cardarelli L, Teyra J, McElroy A, Gross ML, Whelan SPJ, Doench J, Cui X, Brett TJ, Sidhu SS, Virgin HW, Egawa T, Leung DW, Amarasinghe GK, Hartman AL (2021) Lrp1 is a host entry factor for Rift Valley fever virus. Cell 184 (20):5163-5178 e5124. doi:10.1016/j.cell.2021.09.001

13. Devignot S, Sha TW, Burkard TR, Schmerer P, Hagelkruys A, Mirazimi A, Elling U, Penninger JM, Weber F (2023) Low-density lipoprotein receptor-related protein 1 (LRP1) as an auxiliary host factor for RNA viruses. Life Sci Alliance 6 (7). doi:10.26508/lsa.202302005

14. Schwarz MM, Ganaie SS, Feng A, Brown G, Yangdon T, White JM, Hoehl RM, McMillen CM, Rush RE, Connors KA, Cui X, Leung DW, Egawa T, Amarasinghe GK, Hartman AL (2023) Lrp1 is essential for lethal Rift Valley fever hepatic disease in mice. Sci Adv 9 (28):eadh2264. doi:10.1126/sciadv.adh2264

15. Bermudez-Mendez E, Angelino P, van Keulen L, van de Water S, Rockx B, Pijlman GP, Ciuffi A, Kortekaas J, Wichgers Schreur PJ (2023) Transcriptomic Profiling Reveals Intense Host-Pathogen Dispute Compromising Homeostasis during Acute Rift Valley Fever Virus Infection. J Virol 97 (6):e0041523. doi:10.1128/jvi.00415-23

16. de Boer SM, Kortekaas J, Spel L, Rottier PJ, Moormann RJ, Bosch BJ (2012) Acid-activated structural reorganization of the Rift Valley fever virus Gc fusion protein. J Virol 86 (24):13642-13652. doi:10.1128/JVI.01973-12

17. Filone CM, Hanna SL, Caino MC, Bambina S, Doms RW, Cherry S (2010) Rift valley fever virus infection of human cells and insect hosts is promoted by protein kinase C epsilon. PLoS One 5 (11):e15483. doi:10.1371/journal.pone.0015483

18. Harmon B, Schudel BR, Maar D, Kozina C, Ikegami T, Tseng CT, Negrete OA (2012) Rift Valley fever virus strain MP-12 enters mammalian host cells via caveola-mediated endocytosis. J Virol 86 (23):12954-12970. doi:10.1128/JVI.02242-12

19. Dessau M, Modis Y (2013) Crystal structure of glycoprotein C from Rift Valley fever virus. Proceedings of the National Academy of Sciences of the United States of America 110 (5):1696-1701. doi:10.1073/pnas.1217780110

20. Guardado-Calvo P, Atkovska K, Jeffers SA, Grau N, Backovic M, Perez-Vargas J, de Boer SM, Tortorici MA, Pehau-Arnaudet G, Lepault J, England P, Rottier PJ, Bosch BJ, Hub JS, Rey FA (2017) A glycerophospholipid-specific pocket in the RVFV class II fusion protein drives target membrane insertion. Science 358 (6363):663-667. doi:10.1126/science.aal2712

21. Halldorsson S, Behrens AJ, Harlos K, Huiskonen JT, Elliott RM, Crispin M, Brennan B, Bowden TA (2016) Structure of a phleboviral envelope glycoprotein reveals a consolidated model of membrane fusion. Proceedings of the National Academy of Sciences of the United States of America 113 (26):7154-7159. doi:10.1073/pnas.1603827113

22. Hoffmann AB, Mazelier M, Leger P, Lozach PY (2018) Deciphering Virus Entry with Fluorescently Labeled Viral Particles. Methods Mol Biol 1836:159-183. doi:10.1007/978-1-4939-8678-1_8

23. Liu SL, Wang ZG, Xie HY, Liu AA, Lamb DC, Pang DW (2020) Single-Virus Tracking: From Imaging Methodologies to Virological Applications. Chem Rev 120 (3):1936-1979. doi:10.1021/acs.chemrev.9b00692

24. Gu Y, Lozach PY (2023) Illuminating bunyavirus entry into host cells with fluorescence. Mol Microbiol. doi:10.1111/mmi.15165

25. Ouyang T, Liu X, Ouyang H, Ren L (2018) Recent trends in click chemistry as a promising technology for virus-related research. Virus Res 256:21-28. doi:10.1016/j.virusres.2018.08.003

26. Mohl BP, Roy P (2017) Elucidating virus entry using a tetracysteine-tagged virus. Methods 127:23-29. doi:10.1016/j.ymeth.2017.08.004

27. Liu J, Xu M, Tang B, Hu L, Deng F, Wang H, Pang DW, Hu Z, Wang M, Zhou Y (2019) Single-Particle Tracking Reveals the Sequential Entry Process of the Bunyavirus Severe Fever with Thrombocytopenia Syndrome Virus. Small 15 (6):e1803788. doi:10.1002/smll.201803788

28. Sakin V, Paci G, Lemke EA, Muller B (2016) Labeling of virus components for advanced, quantitative imaging analyses. FEBS Lett 590 (13):1896-1914. doi:10.1002/1873-3468.12131

29. Negi G, Sharma A, Chaudhary M, Gupta D, Harshan KH, Parveen N (2023) SARS-CoV-2 Binding to Terminal Sialic Acid of Gangliosides Embedded in Lipid Membranes. ACS Infect Dis 9 (7):1346-1361. doi:10.1021/acsinfecdis.3c00106

30. Lopes MM, Paysan J, Rino J, Lopes SM, Pereira de Almeida L, Cortes L, Nobre RJ (2022) A new protocol for whole-brain biodistribution analysis of AAVs by tissue clearing, light-sheet microscopy and semi-automated spatial quantification. Gene Ther 29 (12):665-679. doi:10.1038/s41434-022-00372-z

31. Nathan L, Daniel S (2019) Single Virion Tracking Microscopy for the Study of Virus Entry Processes in Live Cells and Biomimetic Platforms. Adv Exp Med Biol 1215:13-43. doi:10.1007/978-3-030-14741-9_2

32. Xie E, Ahmad S, Smyth RP, Sieben C (2023) Advanced fluorescence microscopy in respiratory virus cell biology. Adv Virus Res 116:123-172. doi:10.1016/bs.aivir.2023.05.002

33. Stolp B, Melican K (2016) Microbial pathogenesis revealed by intravital microscopy: pros, cons and cautions. FEBS Lett 590 (13):2014-2026. doi:10.1002/1873-3468.12122

34. Ward EN, Pal R (2017) Image scanning microscopy: an overview. J Microsc 266 (2):221-228. doi:10.1111/jmi.12534

35. Combs CA, Shroff H (2017) Fluorescence Microscopy: A Concise Guide to Current Imaging Methods. Curr Protoc Neurosci 79:2 1 1-2 1 25. doi:10.1002/cpns.29

36. Meier R, Franceschini A, Horvath P, Tetard M, Mancini R, von Mering C, Helenius A, Lozach PY (2014) Genome-wide small interfering RNA screens reveal VAMP3 as a novel host

factor required for Uukuniemi virus late penetration. J Virol 88 (15):8565-8578. doi:10.1128/JVI.00388-14

37. Snijder B, Sacher R, Ramo P, Liberali P, Mench K, Wolfrum N, Burleigh L, Scott CC, Verheije MH, Mercer J, Moese S, Heger T, Theusner K, Jurgeit A, Lamparter D, Balistreri G, Schelhaas M, De Haan CA, Marjomaki V, Hyypia T, Rottier PJ, Sodeik B, Marsh M, Gruenberg J, Amara A, Greber U, Helenius A, Pelkmans L (2012) Single-cell analysis of population context advances RNAi screening at multiple levels. Mol Syst Biol 8:579. doi:10.1038/msb.2012.9

38. Sun E, He J, Zhuang X (2013) Live cell imaging of viral entry. Current opinion in virology 3 (1):34-43. doi:10.1016/j.coviro.2013.01.005

39. Laughlin LW, Meegan JM, Strausbaugh LJ, Morens DM, Watten RH (1979) Epidemic Rift Valley fever in Egypt: observations of the spectrum of human illness. Trans R Soc Trop Med Hyg 73 (6):630-633. doi:10.1016/0035-9203(79)90006-3

40. Woelfl F, Leger P, Oreshkova N, Pahmeier F, Windhaber S, Koch J, Stanifer M, Roman Sosa G, Uckeley ZM, Rey FA, Boulant S, Kortekaas J, Wichgers Schreur PJ, Lozach PY (2020) Novel Toscana Virus Reverse Genetics System Establishes NSs as an Antagonist of Type I Interferon Responses. Viruses 12 (4). doi:10.3390/v12040400

41. Pettersson R, Kaariainen L (1973) The ribonucleic acids of Uukuniemi virus, a noncubical tick-borne arbovirus. Virology 56 (2):608-619. doi:10.1016/0042-6822(73)90062-7

42. Mazelier M, Rouxel RN, Zumstein M, Mancini R, Bell-Sakyi L, Lozach PY (2016) Uukuniemi Virus as a Tick-Borne Virus Model. J Virol 90 (15):6784-6798. doi:10.1128/JVI.00095-16

43. Schneider CA, Rasband WS, Eliceiri KW (2012) NIH Image to ImageJ: 25 years of image analysis. Nat Methods 9 (7):671-675. doi:10.1038/nmeth.2089

44. Sbalzarini IF, Koumoutsakos P (2005) Feature point tracking and trajectory analysis for video imaging in cell biology. J Struct Biol 151 (2):182-195. doi:10.1016/j.jsb.2005.06.002

45. Engel S, Heger T, Mancini R, Herzog F, Kartenbeck J, Hayer A, Helenius A (2011) Role of endosomes in simian virus 40 entry and infection. J Virol 85 (9):4198-4211. doi:10.1128/JVI.02179-10

46. Johannsdottir HK, Mancini R, Kartenbeck J, Amato L, Helenius A (2009) Host cell factors and functions involved in vesicular stomatitis virus entry. J Virol 83 (1):440-453. doi:10.1128/JVI.01864-08

Figure legends

Figure 1 – The different fluorescent dyes used to label phenuiviruses. The figure depicts a phenuiviral particle. The different fluorescent dyes used in this chapter to label RVFV, TOSV, and UUKV are also shown. The name of the three viral genomic RNA segments refers to their size as follows: S (small), M (medium), and L (large). Created with BioRender.com.

Figure 2 – Principle of the R18-based fusion assay. After fusion of the viral envelope with endosomal membranes, the self-quenched R18 dye molecules become dequenched and the fluorescence signal dramatically increases. Created with BioRender.com.

Figure 3 – Quantification of viral glycoproteins in virus stocks. (**a**) RVFV was first pelleted through a 25 % (w/v)-sucrose cushion. Then, increasing volumes of the virus stock and known amounts of BSA were separated by nonreducing SDS-PAGE and stained with Coomassie blue. (**b**) The intensity of each band of BSA analyzed in (**a**) was then determined using the gate 'box1' with ImageJ software (values in relative units, RU) and plotted against the corresponding known amount of BSA. The lane "0" in (**a**) served as background, and this value was subtracted from all others. The equation obtained from the linear regression curve of the BSA standard enabled the determination of the RVFV glycoprotein quantity.

Figure 4 – Characterization of fluorescently labeled viral particles. (**a**) The picture shows a sucrose linear gradient after ultracentrifugation. A band that corresponds to RVFV particles labeled with AF546 (RVFV-AF546) is clearly visible at a density in the 35%-40% sucrose

range. (**b**) Pfu assay used for the titration of RVFV-AF546. After 3 days of incubation with different dilutions of the labeled viral particles at 37 °C, Vero cells were stained with a crystal violet solution. The plaques were then revealed after gentle washing and drying. (**c**) The fluorescent particles (RVFV-AF546) were analyzed by nonreducing SDS-PAGE followed by Coomassie blue staining or fluorography. The envelope proteins Gn and Gc were the only fluorescently labeled proteins. (**d**) A confocal microscopy picture of individual RVFV-AF546 particles is shown.

Figure 5 – Fluorescence microscopy to analyze virus motion. (**a**) Vero cells transfected to express PH-PLCΔ1-EGFP, an EGFP-tagged marker in the plasma membrane, were exposed to RVFV-AF546 for 1 h on ice. Next, samples were fixed and imaged with a confocal microscope. The image shows RVFV particles (red arrowheads) on filopodia. (**b**) UUKV labeled with AF647 (UUKV-AF647) was allowed to bind HeLa cells expressing the virus receptor DC-SIGN (HeLa DC-SIGN) in suspension and on ice. Cells were then seeded on coverslips before warming to RT and imaging on the bottom cell surface by TIRF microscopy. UUKV trajectory was recorded at 1/10 Hz and subjected to computational analysis with the Image J-based plugin software Particle Tracker [44] (fuchsia line in the lower right circular box). (**c**) HeLa DC-SIGN cells were exposed to UUKV labeled with AF568 (UUKV-AF568) on ice for 1 h. Then, cells were warmed at 37 °C to trigger endocytosis and imaged by spinning disc confocal microscopy up to 25 min.

Figure 6 – Flow cytometry to measure virus binding and internalization. (**a**) Various amounts of TOSV particles labeled with AF488 particles (TOSV-AF488) were bound to A549 cells on ice, and samples were analyzed by flow cytometry. (**b**) TOSV-AF488 (MOI ~10) was bound to A549 cells on ice before warming to 37 °C for 30 min. Internalization was analyzed by flow cytometry after cell fixation and trypan blue treatment to quench fluorescence due to cell-surface bound viral particles. RFI, relative fluorescence intensity.

Figure 7 – Fluorimetry to quantify virus fusion in cells. The binding of TOSV labeled with R18 (TOSV-R18) was synchronized on ice, and internalization into cells was triggered by rapid warming. The R18 diffusion was quantified by measuring R18 dequenching in living cells (blue curve). In the presence of ammonium chloride (NH_4Cl, red curve), a weak base that neutralizes the intracellular pH, virus fusion is completely blocked. Only free R18 diffusion is measured. The black curve shows the virus fusion-specific R18 release, *i.e.*, blue (fusion + free diffusion) – red (free diffusion). RFI, relative fluorescence intensity.

Dye	Alexa Fluor (AF) succinimidyl esters	Octadecyl rhodamine B chloride (R18)
Virus component targeted	Glycoproteins Gn and Gc	Envelope
React with	Free amine groups	Lipophylic
Emission	From ultraviolet to far red	Yellow

Table 1 – Organic dyes used in this series of protocols. Two types of organic dyes are used in our procedure to make RVFV and other phenuiviruses fluorescent, namely the AF molecules and the lipophilic dye R18.

v = RVFV	RU (from Fig. 3a)	RU - BG	x = y / 74.6 (from Fig. 3b)	x / v ($\mu g.mL^{-1}$)	RVFV ($\mu g.mL^{-1}$ / µM)
15 µL	123.8	62.2	0.83 µg	55.6	74.2 / 1.5
10 µL	105.8	44.2	0.59 µg	59.3	
5 µL	89.9	28.3	0.38 µg	75.9	
2.5 µL	81.4	19.7	0.26 µg	105.9	
0 (BG)	61.6				

Table 2 – Determination of the concentration of the viral glycoproteins Gn and Gc. The intensity of each volume of virus stock analyzed in Fig. 3a was semi-quantified with ImageJ software as relative units (column "RU"). The background (BG) was subtracted from these values (column "RU – BG"). Using the equation defined in Fig. 3b, it was possible to determine the amount of RVFV Gn and Gc (x = y / 74.6) and finally the concentration of the two glycoproteins (x / v). In this example, Gn and Gc are considered as a single glycoprotein, and an average molecular weight of 52 kDa is used to calculate the molarity of both glycoproteins in the virus stock. The left column gives the average concentration ($\mu g.mL^{-1}$) and molarity of RVFV glycoproteins Gn and Gc in the virus stock.

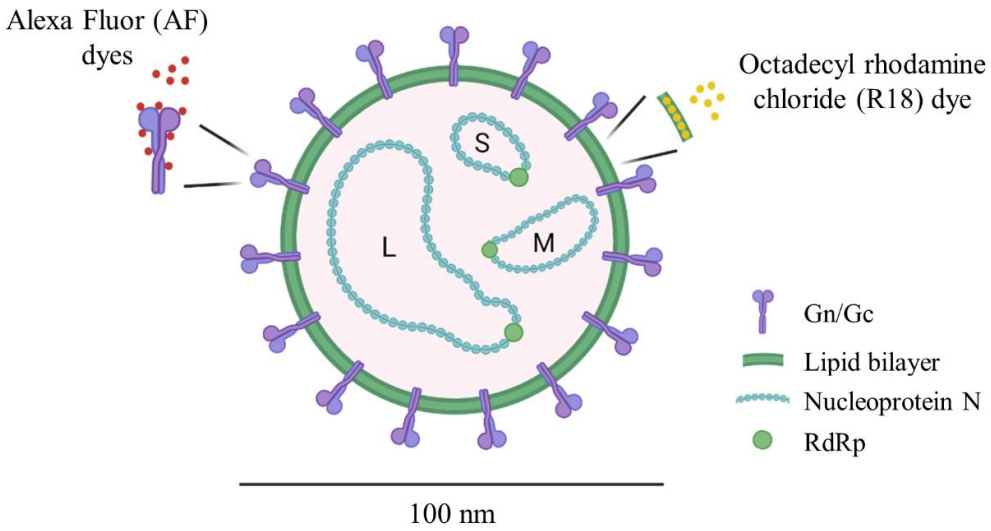
Alexa Fluor (AF)
dyes
Octadecyl rhodamine
chloride (R18) dye
S
L
M
Gn/Gc
Lipid bilayer
Nucleoprotein N
RdRp
100 nm

Fig. 1

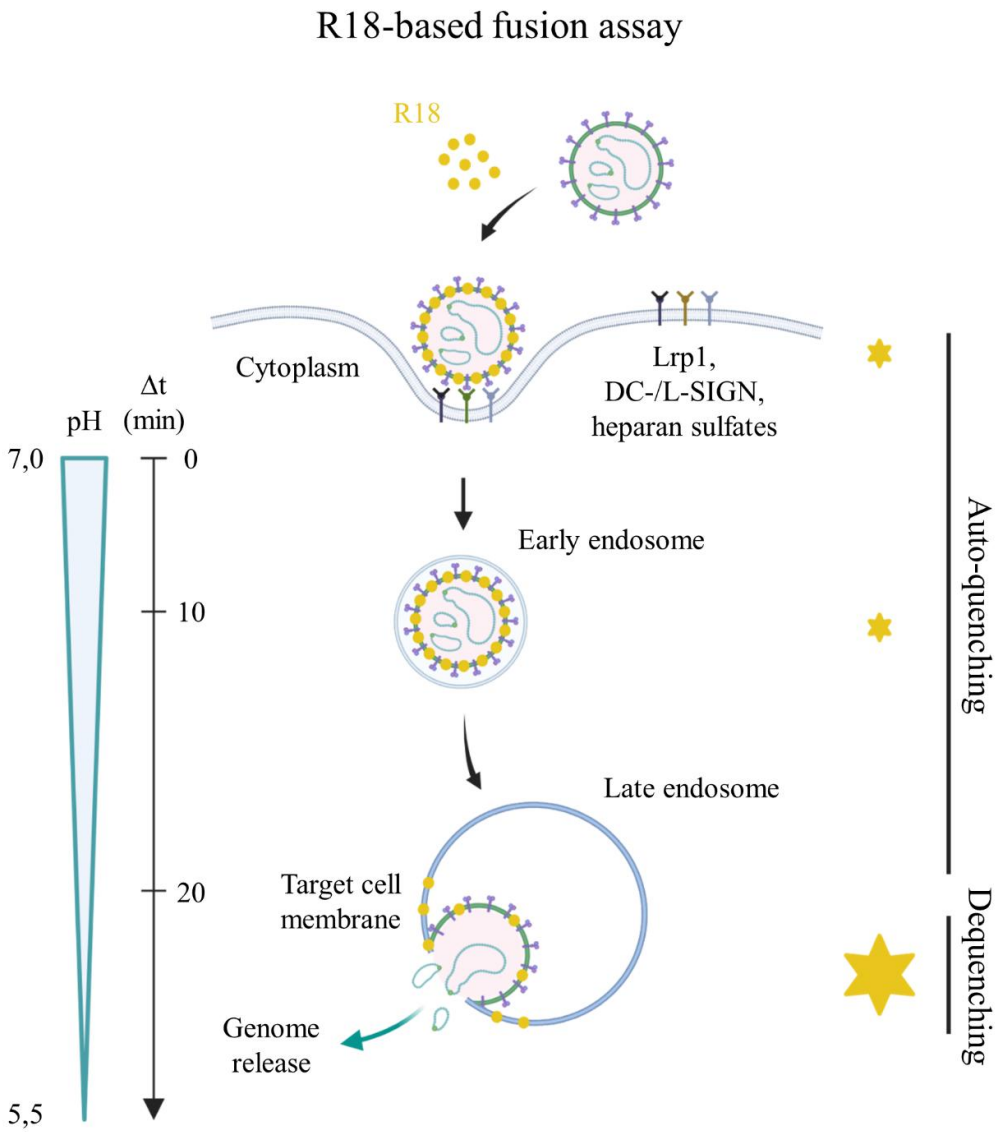
R18-based fusion assay
R18
Cytoplasm
Lrp1,
DC-/L-SIGN,
heparan sulfates
Early endosome
Late endosome
Target cell
membrane
Genome
release
pH
Δt
(min)
7,0
5,5
0
10
20
Auto-quenching
Dequenching

Fig. 2

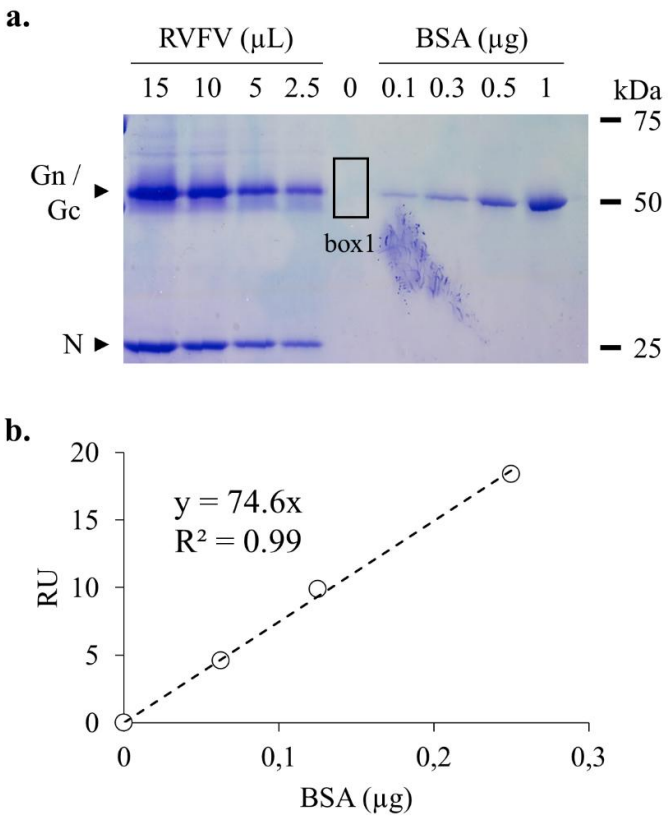
a.
RVFV (µL)
BSA (µg)
15 10 5 2.5 0 0.1 0.3 0.5 1
kDa
75
50
25
Gn / Gc
N
box1
b.
y = 74.6x
R² = 0.99
RU
20
15
10
5
0
0 0,1 0,2 0,3
BSA (µg)

Fig. 3

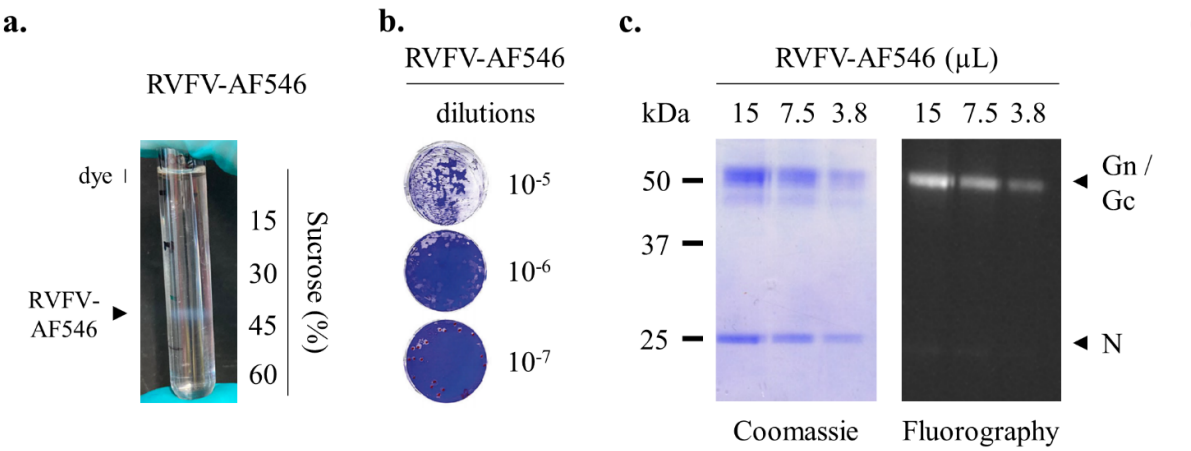
a.
RVFV-AF546
dye
RVFV-AF546
15
30
45
60
Sucrose (%)
b.
RVFV-AF546
dilutions
10-5
10-6
10-7
c.
RVFV-AF546 (µL)
kDa
15 7.5 3.8
15 7.5 3.8
50
37
25
Gn / Gc
N
Coomassie
Fluorography
d.
RVFV-AF546
1 µm

Fig. 4

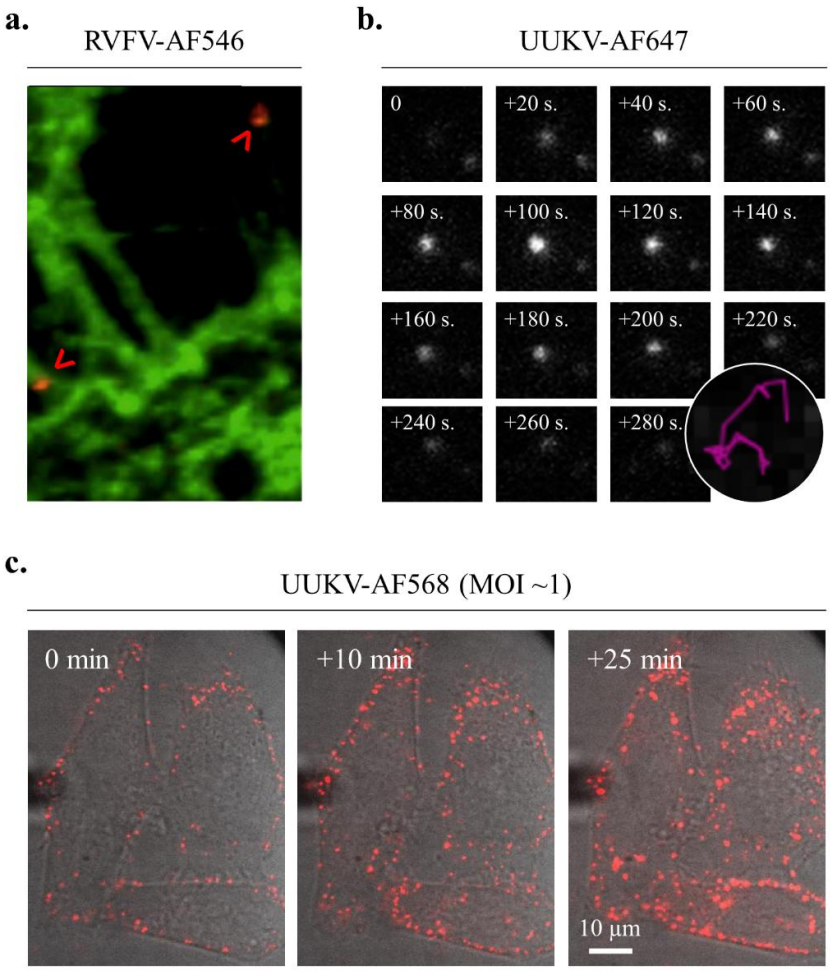
a.
RVFV-AF546
b.
UUKV-AF647
0
+20 s.
+40 s.
+60 s.
+80 s.
+100 s.
+120 s.
+140 s.
+160 s.
+180 s.
+200 s.
+220 s.
+240 s.
+260 s.
+280 s.
c.
UUKV-AF568 (MOI ~1)
0 min
+10 min
+25 min
10 µm

Fig. 5

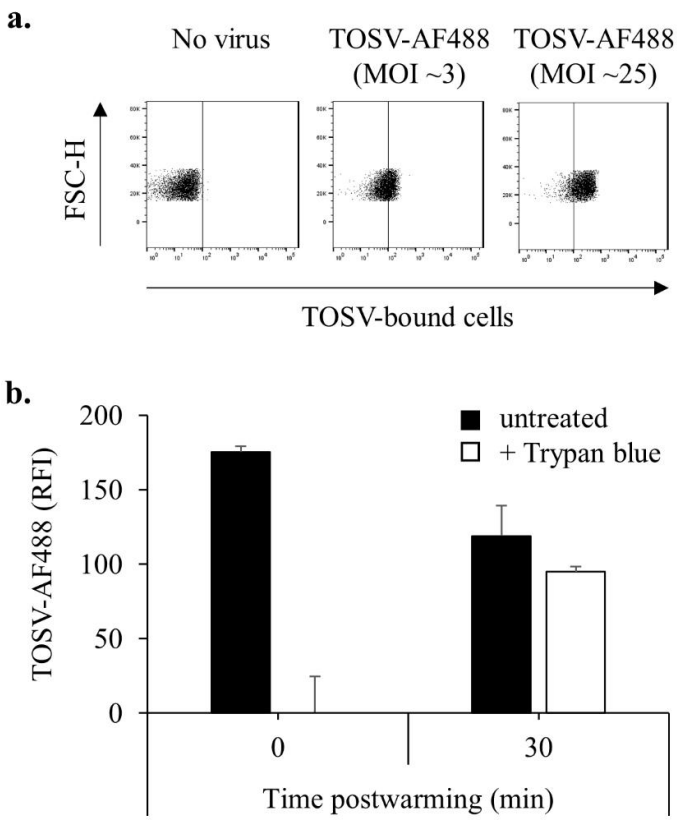
a.
No virus
TOSV-AF488
(MOI ~3)
TOSV-AF488
(MOI ~25)
FSC-H
TOSV-bound cells
b.
TOSV-AF488 (RFI)
200
150
100
50
0
untreated
+ Trypan blue
0
30
Time postwarming (min)

Fig. 6

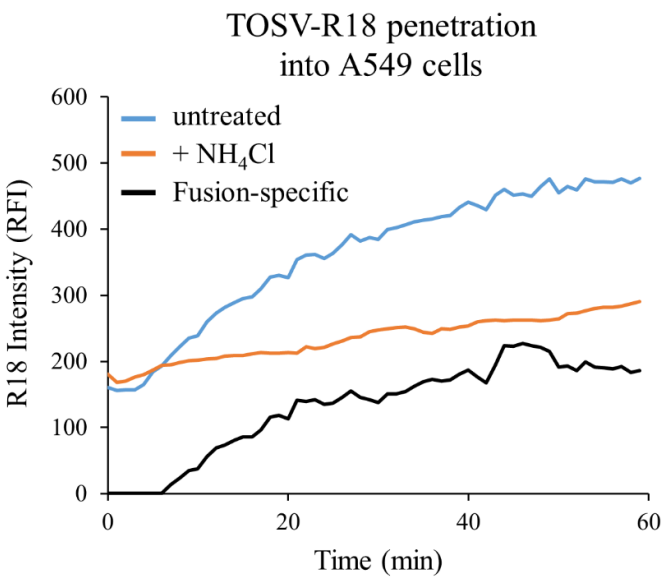
TOSV-R18 penetration
into A549 cells
untreated
+ NH4Cl
Fusion-specific
R18 Intensity (RFI)
600
500
400
300
200
100
0
0
20
40
60
Time (min)

Fig. 7